

# Random forest-based physical activities recognition by using wearable sensors

DOI: 10.35530/IT.073.01.20215

ZHANG JUNJIE  
CAI SHENGAOXU JIE  
YUAN HUA

## ABSTRACT – REZUMAT

### Random forest-based physical activities recognition by using wearable sensors

Physical activity recognition (PAR) is a topic worthy of attention. In order to improve the practicality of wearable sensors for recognition, in this study, we propose an approach to create a classifier of PAR based on the collected data. At first, we discuss how features extracted from the accelerometer and gyroscope contribute to distinguish different activities, including walking, walking upstairs, walking downstairs, sitting, standing, laying, and also provide an analytical method employed for this purpose. Then, a supervised machine learning method, random forest algorithm, is adopted to create a classifier to recognize physical activities based on the extracted features. Lastly, the performances of the constructed classifier are evaluated and compared with other methods. The performance evaluation shows the classifier trained by random forest algorithm are better than other algorithms, and its overall recognition rate reaches 93.75%. In addition, our approach also has strong potential for applications in smart textiles.

**Keywords:** physical activities recognition, random forest, smart textiles, features analysis

### Recunoașterea activităților fizice prin algoritmul arborilor decizionali utilizând senzorii purtabili

Recunoașterea activității fizice (PAR) este un subiect demn de atenție. Pentru a îmbunătăți caracterul practic al senzorilor purtabili pentru recunoaștere, în acest studiu, propunem o abordare pentru a crea un clasificator al PAR pe baza datelor culese de către aceștia. La început, discutăm despre modul în care caracteristicile extrase din accelerometru și giroscop contribuie la distingerea diferitelor activități, inclusiv mersul pe jos, urcarea, coborârea, poziția așezat, statul în picioare, poziția culcat și, de asemenea, oferă o metodă analitică folosită în acest scop. Apoi, o metodă de învățare automată supravegheată, algoritmul arborilor decizionali, este adoptată pentru a crea un clasificator care să recunoască activitățile fizice pe baza caracteristicilor extrase. În final, performanțele clasificatorului construit sunt evaluate și comparate cu alte metode. Evaluarea performanței arată că acest clasificator antrenat de algoritmul arborilor decizionali este mai performant decât alți algoritmi, iar rata sa de recunoaștere globală ajunge la 93,75%. În plus, abordarea noastră are și un potențial puternic pentru aplicații în textilele inteligente.

**Cuvinte-cheie:** recunoașterea activităților fizice, arbori decizionali, textile inteligente, analiza caracteristicilor

## INTRODUCTION

Wearable technologies and smart textiles have gained popularity in recent years, especially for constant supervision of human health or rehabilitation. Some of the related works focused on monitoring body parameters (e.g., blood pressure and heart rate) [1], while some others were absorbed in body posture recognition [2]. By means of wearable technology, another topic worthy of attention is physical activity (e.g., standing, sitting and walking) recognition (PAR), which can also be illustrated as one measure of biomechanical or biomedical tasks of our population as well as body posture [2]. For instance, suggested bending ranges of the human spine are varied with physical activities, hence, whether the spine bending angle is appropriate should be considered together with the physical activity at that time. In order to recognize the physical activity, various approaches have been proposed in the past decades, and most of them were realized by conducting vision computing [3]. Obviously, visual-based

recognition is not suitable for wearable products. Some other works based on audio [4] or radio [5] technologies own potentials for applying to smart textiles, but environment or multi-sensors dependent characteristics discourage users from participating in the PAR [6]. Single or few sensors based wearable technology should be a good choice for PAR with advantages of low-cost, low-energy and low-complexity, and it is most likely to be integrated into textiles. Some previous research utilized an independent accelerometer [7] or a set of accelerometers and gyroscopes embedded in the smartphone [8] with some supervised machine learning algorithms to realize recognition. From the works, we can find that data acquisition by a set of accelerometers and gyroscope, which can be integrated into smart textiles, do contribute to PAR, but data analysis methods can still be improved to promote recognition rates.

In this study, we proposed a new alternative that combines features reduction and random forest algorithm to analyse data from the work of Anguita et al. [8],

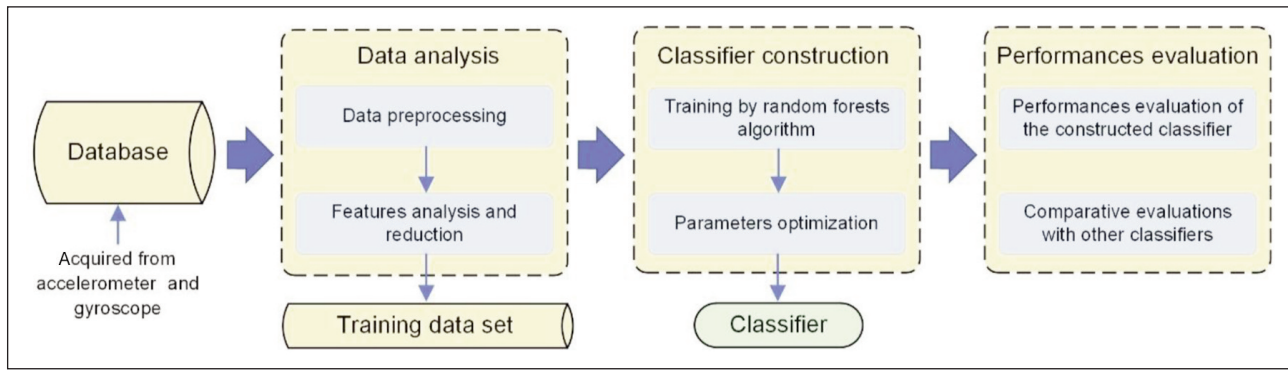


Fig. 1. The flowchart of the proposed methodology

which aims to create a more effective classifier for PAR and improve practicality of wearable accelerometer and gyroscope for PAR. The flowchart of the proposed methodology is shown in figure 1. At first, numerous features extracted from the database are analysed for capabilities of distinguishing different activities (including walking, walking upstairs, walking downstairs, sitting, standing, laying), and the principal features with main contributions to PAR are explored. Then, a supervised machine learning method, random forest (RF) algorithm, is adopted to create a classifier to recognize physical activities based on the extracted features. Lastly, the performances of the constructed classifier are evaluated and compared with other methods to demonstrate the effectiveness of our approach.

## BACKGROUND OF RANDOM FOREST

Random forest, which is a variant of the decision tree-based bagging technique [9], is commonly used for regressions, classifications and cluster problems [10]. The main idea of RF is generating results by a simple unweighted average over a series of independently decision trees [11] that are trained based on samples by sampling with replacement and features by sampling without replacement, as shown in figure 2, and the steps are listed as follow.

1. Randomly draw  $n$  sets of samples from the data set with replacement, and the number of samples in each set is the same with original data set. Meanwhile,  $m$  features in each set are randomly selected from all features without replacement, and features in different sets may be different.

2. Decision trees are grown, based on the corresponding drawn samples and features, in the light of the minimum Gini index as below.

$$I_G(t_{x(x_i)}) = 1 - \sum_{j=1}^M f(t_{x(x_i)}, j)^2 \quad (1)$$

where  $f(t_{x(x_i)}, j)$  denotes the proportion of samples that belongs to the leaf  $j$  while node  $t$  has the value  $x_i$ .

3. The classifier is built on the so-called forest, that is composed of the grown decision trees, by unweighted voting as below

$$\bar{T}(x) = \frac{1}{N} \sum_{k=1}^N T_k \quad (2)$$

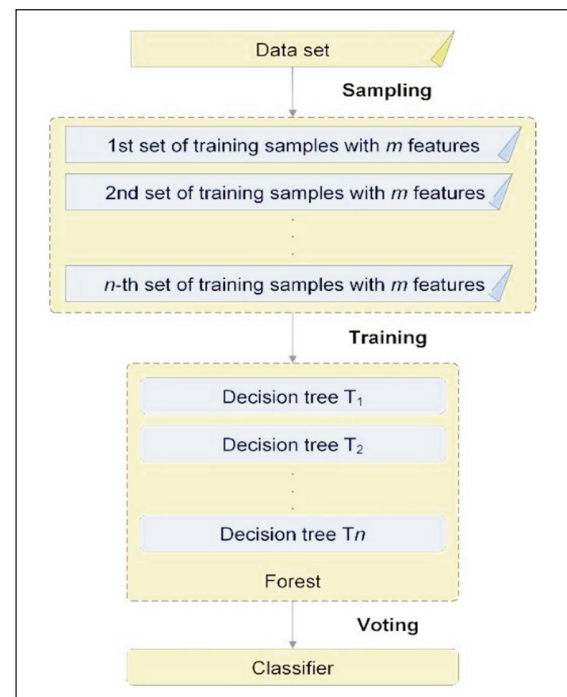


Fig. 2. The flowchart of random forest

where  $T_k$  indicates the  $k$ -th decision tree.

## FEATURES ANALYSIS

### Data acquisition and pre-processing

In this study, the adopted human activity recognition data set was created by Anguita et al. [8]. All data, in terms of 3-axial linear acceleration and 3-axial angular velocity at a constant rate of 50 Hz, came from the accelerometer and gyroscope embedded in smartphones worn on the waist by 30 volunteers, who are in an age bracket of 19–48 years. The collected data went through a transformation process, including noise filtering, time-domain analysis and frequency domain analysis, and 35 kinds of signals were obtained as listed in table 1. Then, a set of 561 features were estimated from these signals by conducting a series of mathematical operations listed in table 2. For examples, body acceleration signals in X direction ('tBodyAcc-X' in table 1) can be averaged ('mean()' in table 2) to generate a feature named 'tBodyAcc-mean()-X'.

Table 1

DESCRIPTION FOR OBTAINED SIGNALS		
Code	Name	Descriptions
0-2	tBodyAcc-XYZ	X,Y,Z-dimensional time domine signals of body linear acceleration
3-5	tGravityAcc-XYZ	X,Y,Z-dimensional time domine signals of acceleration of gravity
6-8	tBodyAccJerk-XYZ	X,Y,Z-dimensional time domain signals of body linear jerk
9-11	tBodyGyro-XYZ	X,Y,Z-dimensional time domain signals of body angular velocity
12-14	tBodyGyroJerk-XYZ	X,Y,Z-dimensional time domain signals of body angular jerk
15	tBodyAccMag	Magnitude of three-dimensional time domine signals of body linear acceleration was calculated by conducting Euclidean norm
16	tGravityAccMag	Magnitude of three-dimensional time domine signals of acceleration of gravity was calculated by conducting Euclidean norm
17	tBodyAccJerkMag	Magnitude of three-dimensional time domine signals of body linear jerk was calculated by conducting Euclidean norm
18	tBodyGyroMag	Magnitude of three-dimensional time domine signals of body angular velocity was calculated by conducting Euclidean norm
19	tBodyGyroJerkMag	Magnitude of three-dimensional time domine signals of body angular jerk was calculated by conducting Euclidean norm
20-22	fBodyAcc-XYZ	X,Y,Z-dimensional frequency domine signals of body linear acceleration
23-25	fBodyAccJerk-XYZ	X,Y,Z-dimensional frequency domain signals of body linear jerk
26-28	fBodyGyro-XYZ	X,Y,Z-dimensional frequency domain signals of body angular velocity
29-31	fBodyGyroJerk-XYZ	X,Y,Z-dimensional frequency domain signals of body angular jerk
32	fBodyAccMag	Magnitude of three-dimensional frequency domine signals of body linear acceleration was calculated by conducting Euclidean norm
33	fBodyAccJerkMag	Magnitude of three-dimensional frequency domine signals of body linear jerk was calculated by conducting Euclidean norm
34	fBodyGyroMag	Magnitude of three-dimensional frequency domine signals of body angular velocity was calculated by conducting Euclidean norm
35	fBodyGyroJerkMag	Magnitude of three-dimensional frequency domine signals of body angular jerk was calculated by conducting Euclidean norm

Table 2

DESCRIPTION FOR SIGNAL OPERATORS		
Code	Name	Descriptions
1	mean( )	Mean value
2	std( )	Standard deviation
3	mad( )	Median absolute deviation
4	max( )	Largest value in array
5	min( )	Smallest value in array
6	sma( )	Signal magnitude area
7	energy( )	Energy measure. Sum of the squares divided by the number of values.
8	iqr( )	Interquartile range
9	enentropy( )	Signal entropy
10	arCoeff( )	Autoregression coefficients with Burg order equal to 4
11	correlation( )	Correlation coefficient between two signals
12	maxInds( )	Index of the frequency component with the largest magnitude
13	meanFreq( )	Weighted average of the frequency
14	skewness( )	Skewness of the frequency domain signal
15	kurtosis( )	Kurtosis of the frequency domain signal
16	bandsEnergy( )	Energy of a frequency interval within the 64 bins of the FFT of each window
17	angle( )	Angle between to vectors

Meanwhile, human activities were also recorded by video, which were utilized for labelling acquired data. 10297 items of activities were labelled and classified into six categories in terms of laying (1944 items), standing (1906 items), sitting (1777 items), walking (1722 items), walking upstairs (1542 items), walking downstairs (1406 items). In a word, there are 10297 items of labelled activities with 561 features for descriptions in the data set.

### Features analysis and reduction

More features would boost the potential for discriminating different physic activities, but they also increase the computational load. In order to reduce computational load without decreasing the ability of PAR, the validity of features was verified at first, and useless features were eliminated.

In the verification, histograms were utilized to visualize descriptive characteristics of the features for different activities. Abscissa and ordinate in the histogram respectively indicate the normalized value of the selected feature and a corresponding number of activities, while different types of activities are discriminated by colours. From the histograms of some features, we can find that distributions of some types of activities are significantly different from others, and it means these types of activities can be recognized by the features. For example, as shown in figure 3, the feature “angle(X,gravityMean)” is particularly suitable for distinguishing ‘laying’ from other activities, and the feature “fBodyAcc-entropy()-X” can be used for distinguishing between static activities (i.e., “sitting”,

“standing” and “laying”) and dynamic activities (i.e., “walking”, “walking upstairs” and “walking downstairs”). By contrast, some features are hardly utilized for recognition due to similarities of different distributions in the histograms, some distributions are so similar that the corresponding feature cannot own the ability of recognition, such as the features “fBodyBodyGyroJerkMag-kurtosis()” and “fBodyBodyGyroMag-skewness()” in figure 4. The similarity of any two distributions in the histogram of a feature be quantitatively measured by equation 3.

$$S = \frac{\sum_{i=1}^N [(H_1(i) - \bar{H}_1) \cdot (H_2(i) - \bar{H}_2)]}{\sqrt{\sum_{i=1}^N (H_1(i) - \bar{H}_1)^2 \cdot \sum_{i=1}^N (H_2(i) - \bar{H}_2)^2}} \quad (3)$$

where  $N$  denotes the number of activities (i.e., ordinate value) corresponding to the  $i$ -th bin (range of abscissa value are divided into  $N$  bins) in the distribution 1, and  $\bar{H}$  is the mean values calculated as below.

$$\bar{H} = \frac{\sum_{i=1}^N H_1(i)}{N} \quad (4)$$

In equation 3,  $S$  approaching 1 indicates the greater the correlation between the two distributions, and if  $S$  is negative, it indicates that the feature has a strong ability to distinguish between the two distributions. Thus, by pairwise comparison of the distributions caused by six types of activities in the histogram of a feature, we can generate the confusion matrix of similarities for judging the ability of PAR of the feature, as shown in figure 3 and 4. After analysis, 64 features were eliminated because of low contributions to PAR.

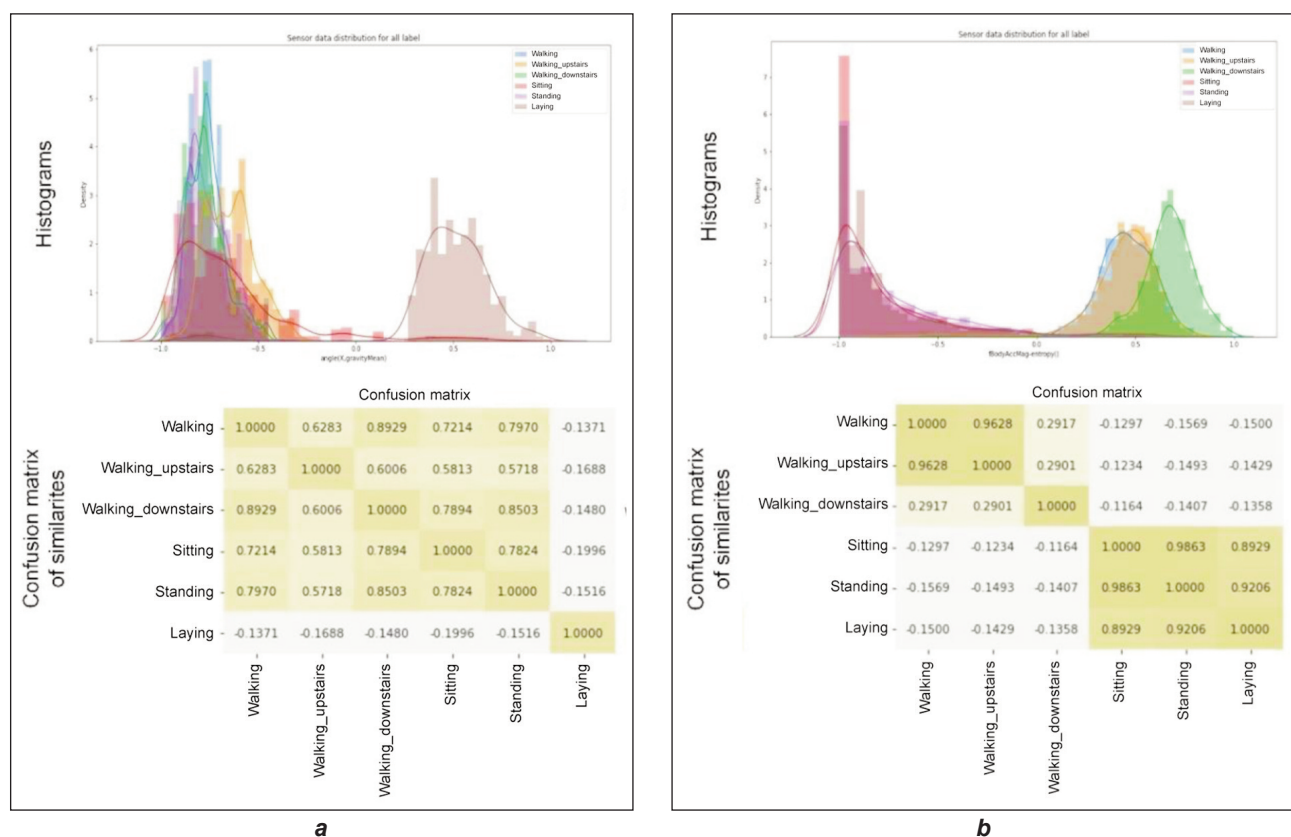


Fig. 3. Histograms and confusion matrix of similarities of the features with high contributions to PAR, including: a – angle(X,gravityMean); b – fBodyAcc-entropy()-X

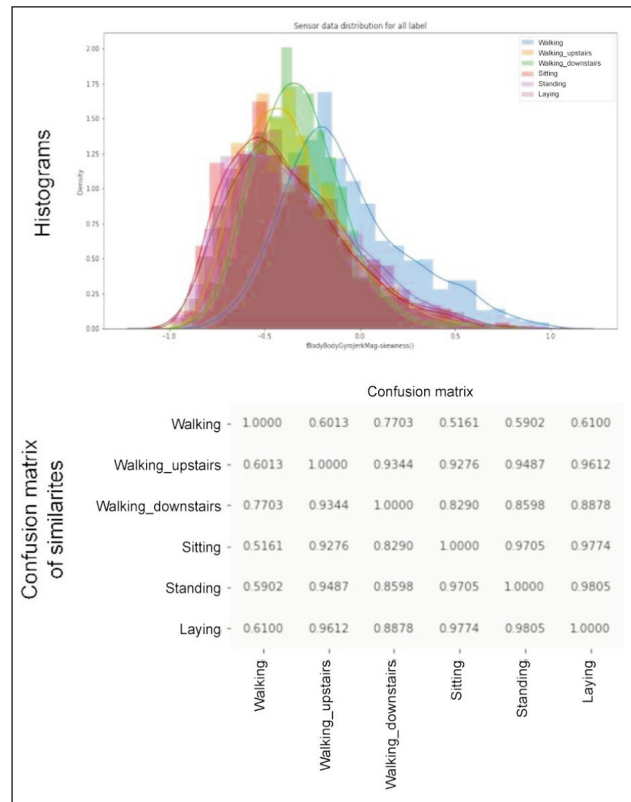
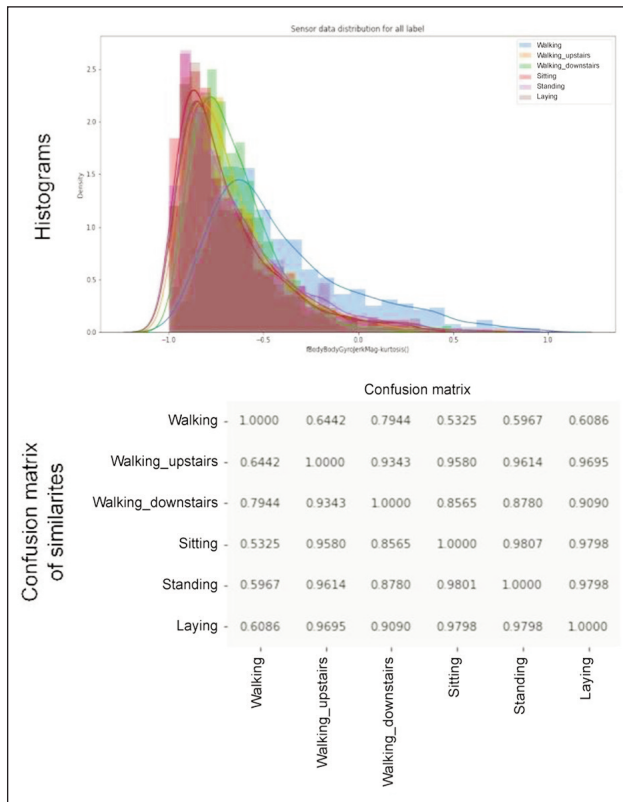


Fig. 4. Histograms and confusion matrix of similarities of the features with low contributions to PAR, including: a – fBodyBodyGyroJerkMag-kurtosis(); b – fBodyBodyGyroMag-skewness()

## CLASSIFIER CONSTRUCTION AND EVALUATION

In the construction of the classifier, at first, the obtained data set is divided into a training subset and test subset according to the ratio of 7:3. Next, based on the training subset, parameters of random forest algorithm were optimized to generate a classifier for PAR. Then, the performance of the classifier was evaluated based on test subset. Finally, a comparison experiment with other commonly used classifiers, including support vector machines (SVM) [12], k-nearest neighbour classification(KNN) [13], multi-layer perceptron (MLP) [14] and quadratic discriminant analysis (QDA) [15], was conducted. The detailed descriptions are given in the following subsections.

### Classifier training by random forest

The classifier for PAR was trained by random forest algorithm based on training subset. During the training process, two important parameters, including the number of decision trees  $n_{tree}$ , and the max number of features used for growing a tree  $max\_features$ , need to be determined. In usual,  $max\_features$  is decided by “sqrt” or “log2”, in other words,  $max\_features$  can be square root or base 2 logarithm of total number of features, and which one is better needs to be compared. The optimal value of  $n_{tree}$  can be achieved by traversing possible values. Thus, as shown in figure 5, we have plotted curves that reflect

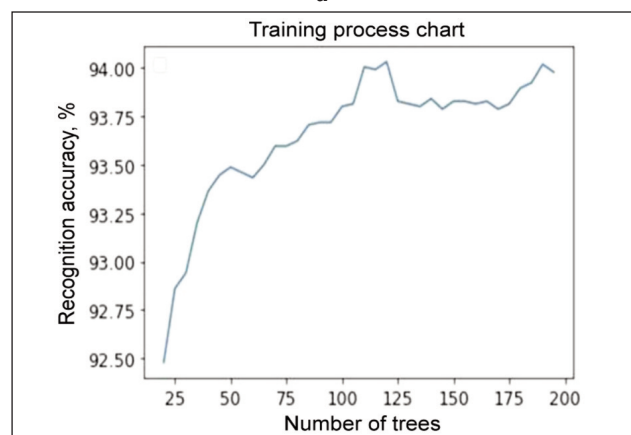
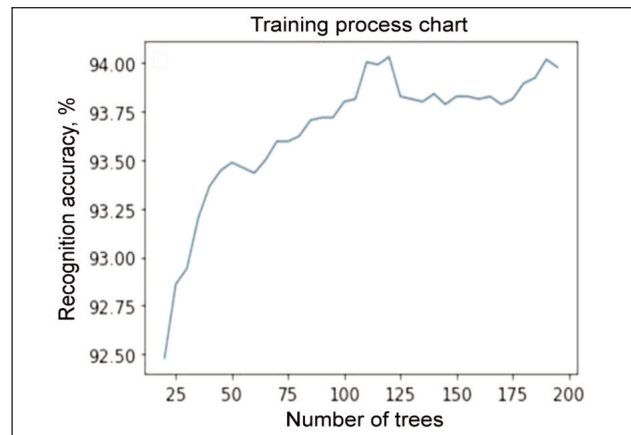


Fig. 5. Iteration curves of training by random forest with different max\_features decided by: a – “log2”; b – “sqrt”

the training accuracy varies with the  $n\_tree$  respectively under the  $max\_features$  determined by “sqrt” and “log2”.

Table 3

RECOGNITION RATES OF THE ACTIVITIES		
Labels	Number of samples	Recognition rate (%)
Laying	537	100
Standing	533	97.00
Sitting	490	89.80
Walking	496	97.58
Walking upstairs	471	92.57
Walking downstairs	420	83.09

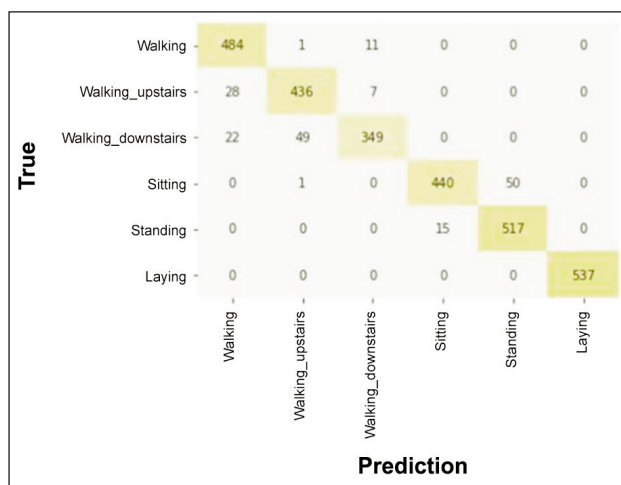


Fig. 6. Confusion matrix of prediction performance

Table 4

COMPARISON RESULTS OF CLASSIFIERS TRAINED BY DIFFERENT ALGORITHMS					
Indicator	RF	SVM	KNN	MLP	QDA
Recognition rate	93.34%	91.49%	87.37%	89.57%	78.78%

From the curves, we can find that the best recognition rate is 94.03% corresponding to  $n\_tree = 120$  on the conditions of  $max\_features$  decided by “log2”, while the best recognition rate is 93.24% corresponding to  $n\_tree = 125$  on the conditions of  $max\_features$  decided by “sqrt”. Obviously, the curve from figure 5, a can achieve better result than curve from figure 5, b. Thus, the optimized parameters can be determined as follow:  $n\_tree = 125$ ;  $max\_features = \text{round}(\log_2 497) = 9$ , where 497 derives from that 561 (total number of features) subtracts 64 (eliminated features).

### Performance evaluation

Through the application of the trained classifier on the test subset, we find that the overall recognition rate of the classifier reached 93.75%, of which the recognition rates for the six physical activities are listed in table 3, and more details are presented by the confusion matrix as shown in figure 6.

The test results show that the classifier has achieved a good recognition rate for dynamic activities, static activities, and single-type activity. Among them, the trained classifier has the best ability to recognize “laying”, and the recognition rates of “standing”, “walking” and “walking upstairs” are all above 90%, while the recognition rate of “sitting” is approximate to 90%. Although the recognition rate of “Walking downstairs” is only 83.09%, it is still at a relatively high level. In addition, the recognition rate of the classifier on the test subset is close to the recognition rate on the training subset, which indicates the trained classifier has a strong generalization ability.

In order to further evaluate the performances of the classifier, we compare the current classifier with the classifiers trained by other common algorithms, including SVM, KNN, MLP and QDA, based on the

same training set. The comparison result is listed in table 4.

From the results, it is easy to find that the classifier trained by random forest has better performances than others.

### CONCLUSIONS

In order to improve the practicality of wearable accelerometers and gyroscopes for physical activities recognition, we have proposed an approach that combines features reduction and random forest algorithm to boost the recognition rate. The test has shown the classifier trained by random forest algorithm are better than other algorithms, and its overall recognition rate reaches 93.75% which means this kind of scheme has strong feasibility.

In addition, wearable accelerometers and gyroscopes can be integrated into smart textiles, some examples were created by other researchers [16, 17], which means our approach has strong potential for applications in smart textiles. It is worth mentioning that data and features for recognitions should be different if wearable sensors are embedded in the smart textiles placed on different parts of the body, but we think our approach can still deal with them and achieve a good result.

Therefore, in the future, works can be focused on the following aspects.

1. Make a series of wearable sensors embedded in smart textiles and collect more data from them to prove the feasibility of applications in smart textiles and further improve the recognition rate of the classifier.
2. Pay attention to recognize other physical activities besides the six existing ones, such as running and jumping.

## ACKNOWLEDGEMENTS

This research was supported by the funds from National Scientific Research Project of Hubei Provincial Department Key R&D Program of China (No: 2019YFB1706300), and of Education, China (No: Q20191707).

## REFERENCES

- [1] Quandt, B.M., Scherer, L.J., Boesel, L.F., Wolf, M., Bona, G.L., Rossi, R.M., *Body-Monitoring and Health Supervision by Means of Optical Fiber-Based Sensing Systems in Medical Textiles*, In: *Advanced Healthcare Materials*, 2015, 4, 3, 330–355
- [2] Abro, Z.A., Zhang, Y.F., Chen, N.L., Hong, C.Y., Lakho, R.A., Halepoto, H., *A novel flex sensor-based flexible smart garment for monitoring body postures*, In: *Journal of Industrial Textiles*, 2019, 49, 2, 262–274
- [3] Jalal, A., Kim, Y.H., Kim, Y.J., Kamal, S., Kim, D., *Robust human activity recognition from depth video using spatiotemporal multi-fused features*, In: *Pattern Recognition*, 2017, 61, 295–308
- [4] Chahuara, P., Fleury, A., Vacher, M., *On-line human activity recognition from audio and home automation sensors: comparison of sequential and non-sequential models in realistic smart homes*, In: *Journal of Ambient Intelligence & Smart Environments*, 2016, 8, 4, 399–422
- [5] Wang, S., Zhou, G., *A review on radio-based activity recognition*, In: *Digital Communications & Networks*, 2015, 1, 1, 20–29
- [6] Voicu, R.A., Dobre, C., Bajenaru, L., Ciobanu, R.I., *Human physical activity recognition using smartphone sensors*, In: *Sensors*, 2019, 19, 3, 458
- [7] Mannini, A., Sabatini, A.M., *Machine learning methods for classifying human physical activity from on-body accelerometers*, In: *Sensors*, 2010, 10, 2, 1154–1175
- [8] Anguita, D., Ghio, A., Oneto, L., Parra, X., Reyes-Ortiz, J.L., *A Public Domain Dataset for Human Activity Recognition Using Smartphones*, In: *21th European Symposium on Artificial Neural Networks, Computational Intelligence and Machine Learning, ESANN 2013, Bruges, Belgium, 24–26 April 2013*, Available at: <http://archive.ics.uci.edu/ml/datasets/Human+Activity+Recognition+Using+Smartphones> [Accessed on January 27, 2021]
- [9] Dietterich, T.G., *An experimental comparison of three methods for constructing ensembles of decision trees: bagging, boosting, and randomization*, In: *Machine Learning*, 2000, 40, 2, 139–157
- [10] He, Z., Tran, K.-P., Thomassey, S., Zeng, X., Xu, J., Yi, C.H., *Modeling color fading ozonation of reactive-dyed cotton using the Extreme Learning Machine, Support Vector Regression and Random Forest*, In: *Textile Research Journal*, 2020, 90, 7–8, 896–908
- [11] Myles, A.J., Feudale, R.N., Liu, Y., Woody, N.A., Brown, S.D., *An introduction to decision tree modelling*, In: *Journal of Chemometrics*, 2004, 18, 6, 275–285
- [12] Andrew, A.M., *An introduction to support vector machines and other kernel-based learning methods*, In: *Kybernetes*, 2001, 32, 1, 1–28
- [13] Kramer, O., *K-nearest neighbors*, In: *Intelligent Systems Reference Library*, 2013, 41, 2, 13–23
- [14] Rynkiewicz, J., *Introduction to multilayer perceptron and hybrid hidden Markov models*, In: Lesage, C., Cottrell, M. (eds) *Connectionist Approaches in Economics and Management Sciences. Advances in Computational Management Science*, Springer, Boston, 2003, 6
- [15] James, G., Witten, D., Hastie, T., Tibshirani, R., *An Introduction to Statistical Learning: With Applications in R*, Springer Texts in Statistics, 2013, 149–151.
- [16] Younes, R., Hines, K., Forsyth, J., Dennis, J., Martin, T., Jones, M., *The design of smart garments for motion capture and activity classification*, In: *Smart Textiles and their Applications*, 2016, 627–655
- [17] Li, M., Torah, R., Nunes-Matos, H., Wei, Y., Beeby, S., Tudor, J., Yang, K., *Integration and Testing of a Three-Axis Accelerometer in a Woven E-Textile Sleeve for Wearable Movement Monitoring*, In: *Sensors*, 2020, 20, 18, 5033

---

### Authors:

ZHANG JUNJIE<sup>1</sup>, CAI SHENGHAO<sup>1</sup>, XU JIE<sup>2</sup>, YUAN HUA<sup>3</sup>

<sup>1</sup>Engineering Research Center of Hubei Province for Clothing Information, School of Mathematics and Computer Science, Wuhan Textile University, 430073 Wuhan, China

<sup>2</sup>School of Textile Science and Engineering, Wuhan Textile University, 430073 Wuhan, China

<sup>3</sup>Wuhan Textile and Apparel Digital Engineering Technology Research Center, School of fashion, Wuhan Textile University, 430073, Wuhan, China

### Corresponding authors:

XU JIE

e-mail: [jxu@wtu.edu.cn](mailto:jxu@wtu.edu.cn)

YUAN HUA

e-mail: [2019009@wtu.edu.cn](mailto:2019009@wtu.edu.cn)